

THICKNESS INFLUENCE ON THE PYROELECTRIC SIGNAL OF DOPPED PZT CERAMIC PELLETS

V. STANCU, M. BOTE^{*}, L. AMARANDE, L. PINTILIE

National Institute of Materials Physics, Atomistilor 405A, 077125 Magurele, Ilfov Romania

$\text{Pb}_{0.98}\text{Bi}_{0.02}\text{Zr}_{0.5}\text{Fe}_{0.1}\text{Nb}_{0.09}\text{Ti}_{0.31}\text{O}_3$ (PBiZFNT) powder obtained by a solid state reaction technique was uniaxial pressed and sintered at 1200°C in order to fabricate dense thin disk ceramics with different thickness (200µ up to 600µm). The pyroelectric response was influenced by the thickness of the ceramics. The thin ceramic disks of 250 µm thickness show better pyroelectric signal (≈35 mV) which recommend them for potential use in laser energy meters.

(Received May 5, 2020; Accepted August 14, 2020)

Keywords: PBiZFNT, Pyroelectric coefficient, Thickness influence

1. Introduction

Pyroelectric materials are very important because they can generate an electrical response upon a temperature change. Since the discovery of a large piezoelectric and pyroelectric effect, lead-based oxide materials are the most widely-used traditional pyroelectric materials [1,2,3]. The research interests has been concentrated on investigation and optimization of the pyroelectric properties [4,5], and on the preparation and characterization of pyroelectric active elements, in the form of bulk ceramics [6,7,8] or thin film samples [9, 10]. Important for pyroelectric application is the relation between sample properties and the electrode exposed to IR radiation. The latest research shows that the carbon electrode is a good candidate because it has good electrical and thermal conductivity, with good transfer of charges and heat [11,12]. Another important aspect is the relation between the size of the pyroelectric element and the magnitude of the pyroelectric signal. In this context, thickness is important to have a good heat transfer and to maximize the temperature variation, with effect on the magnitude of the pyroelectric signal.

In this paper we study the influence of the thickness on the amplitude of the pyroelectric signal generated by $\text{Pb}_{0.98}\text{Bi}_{0.02}\text{Zr}_{0.5}\text{Fe}_{0.1}\text{Nb}_{0.09}\text{Ti}_{0.31}\text{O}_3$ (PBiZFNT) ceramic disks with carbon top electrode. The aim is to establish the optimum thickness for high pyroelectric response.

2. Experimental section

Lead zirconate titanate ceramic doped with bismuth, iron and niobium ($\text{Pb}_{0.98}\text{Bi}_{0.02}\text{Zr}_{0.5}\text{Fe}_{0.1}\text{Nb}_{0.09}\text{Ti}_{0.31}\text{O}_3$, PBiZFNT) was prepared by the solid state synthesis method. All raw materials have a purity greater than 99% and are purchased from Merck or Fluka. Ethanol 99,6% (Chimopar) was used as solvent. The ceramics were prepared according to the procedure presented in Fig. 1. Raw materials were mixed in a RETSCH planetary ball mill at 300 rpm for 2 hours for good homogenization. The PBiZFNT powder was dried at 150°C and calcined at 900°C for 2 hours. The 35 mm diameter PBiZFNT ceramic disks were obtained by cold pressing, while applying an equivalent force of 7 tones. The sintered step was done at 1200°C/ 2 hours (2°C/min heating rate). In this way, compact ceramics with density ~7.3 g/cm³ were obtained. The morphology of PBiZFNT ceramics was studied by using a Tescan Lyra 3XMU scanning electron

* Corresponding author: mihaela.botea@infim.ro

microscope (SEM). The crystal structure was analyzed by X-ray Diffraction (XRD) using a Bruker D8 Advance equipment (powder setting). The ceramic was then cut and polished to obtain disks of different thicknesses. These were covered with silver paste and poled in a silicone oil bath by applying a dc field of 7 kV/mm. At the end, the disks were glued with silver paset on metal supports of 35 mm diameter and 30 mm thickness, playing the role of heat sinks. The free surface was covered with a carbon layer obtained from ccommercial carbon paste (Electrodag PF-407C from Loctite), to increase the emissivity of the surface exposed to IR beam close to the unity. The carbon layer can play also the role of the top electrode.

The frequency dependence of the pyroelectric signal was recorded for different thicknesses of the PBiZFNT ceramic disks, using as an IR source a laser diode M9_808_0150 from Thorlabs, wavelength 808 nm, maximum power 150 mW. The laser beam was electronically modulated using a Tektronix AFG 3052C signal generator, and the pyroelectric signal was recorded using a SR 830 DSP lock-in amplifier, from Stanford Research.

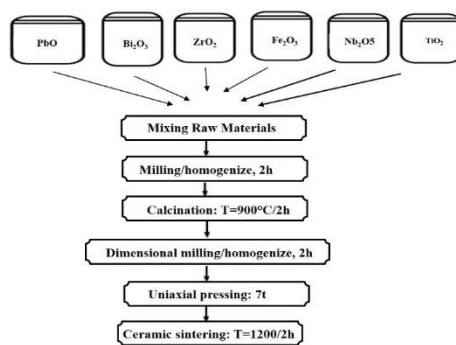


Fig. 1. Flow diagram for the solid state processing of PBiZFNT ceramics.

3. Results and discussion

The morphology of PBiZFNT ceramic disks with different thicknesses obtained by optical polish (from 250 to 600 μm) is illustrated in SEM images (Fig. 2). The addition of the three dopants in the PZT matrix has a significant impact on microstructure. One can observe that the grains are uniformly distribute in the disk, with 3.87 μm average size, the structure is smooth, crack free and dense but there are small pores between grains. These pores may be the result of small bismuth content [13]. The graine size is a consequence of the dopants: bismuth decrease the size and the presence of iron in a larger proportion than niobium leads to increase the size [8,13,14].

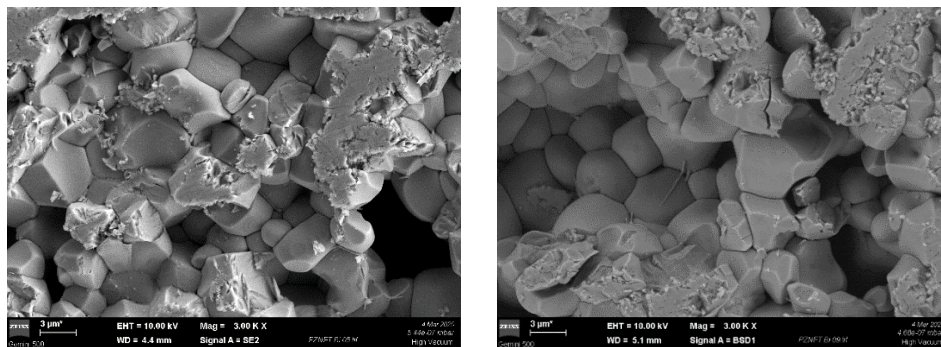


Fig. 2. SEM images of PBiZFNT ceramic disc with 250 μm thickness.

The crystallinity of PBiZFNT ceramics was analyzed by XRD and the peaks were indexed according to ICDD 00-057-0525 and 00-003-0515 patterns (Figure 3). The ceramic disks

show predominantly a PZT tetragonal phase with characteristic peaks at 21.79° , 31.02° , 38.26° and 44.47° corresponding to (100), (101), (111) and (200) crystal planes and a secondary phase of ZrO_2 with a small peak at 28.4° . The presence of bismuth, iron and niobium is marked by the splitting of (200) and (211) peaks [13,14].

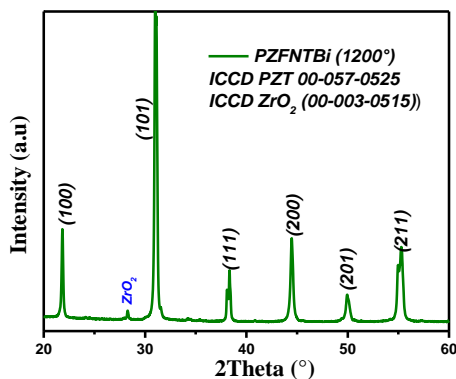


Fig. 3. XRD pattern of PZFNT ceramics sintered at $1200^\circ\text{C}/2\text{h}$.

The typical frequency dependencies for the pyroelectric signal are shown in Fig. 4. The pyroelectric signal was measured directly from the pyroelectric element, in this case ceramic disks with a diameter of 35 mm and different thicknesses ($250\ \mu\text{m}$ up to $600\ \mu\text{m}$) mounted on metal supports.

If the same heat source is applied to a pyroelectric device, the rate of the temperature variation in the pyroelectric device differs by changing the thickness of the pyroelectric element, thus by changing its thermal capacity. Other elements affecting the pyroelectric signal are the material composition, radiation absorption coefficient, the dielectric constant, and the pyroelectric coefficient [15].

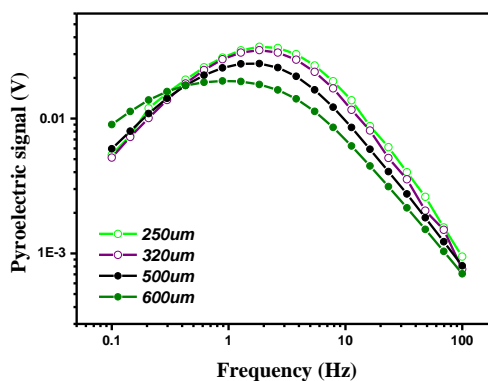


Fig. 4. Frequency dependence of the pyroelectric signal for different thickness of PBiZFNT disks.

One can observe three distinct behaviors: an increasing part at low frequencies, when the temperature variation is limited by heat losses at the back electrode and support; a small plateau when the penetration depth of the heat wave is approximately the same with the thickness of the pyroelectric element; a decreasing part at high frequencies, when the heat wave penetrates on a distance smaller than the thickness of the ceramic disk.

The pyroelectric signal is approximately the same at low frequencies, and decreases for higher thicknesses when the frequency increases above 1 Hz. This is due the same amount of incident energy used to heat samples of different thicknesses, thus with different thermal capacities, leading to smaller temperature variations as the thickness increases. The signals become similar at high frequencies irrespective of thickness, due to the non-uniform heating, thus the

heated layer at the surface will have the same thickness although the total thicknesses of the disks are different [15,16,17]. The results presented in Fig. 4 show that the thickness has impact on the magnitude of the pyroelectric signal only at frequencies in the proximity of maximum (plateau region). One can also see that the frequency domain corresponding to these plateau shifts to higher values as the thickness decreases. This is because the thermal time constant is lower for smaller thicknesses.

The basic equation for the pyroelectric signal is [18,19]:

$$S(\omega) = \frac{\omega \eta p A P_{inc}}{G_T G_e (1 + \omega^2 \tau_T^2)^{1/2} (1 + \omega^2 \tau_e^2)^{1/2}}, \quad (1)$$

in which are defined the pyroelectric signal (S); pulsation ($\omega = 2\pi f$) of the incident radiation on the pyroelectric element, where f is the the modulation frequency of the IR beam; incident power (P_{inc}) on the active element; emissivity (η) of the electrode exposed to IR radiation; pyroelectric coefficient (p); area of the sample (A); thermal conductance (G_T); electric conductance (G_e); thermal time constant ($\tau_T = C_T/G_T$), where C_T is the thermal capacity of the pyroelectric element, and the electrical time constant ($\tau_e = C_e/G_e$), where C_e is the capacitance of the pyroelectric element.

A significant parameter to evaluate the pyroelectric properties is the total pyroelectric coefficient, given by the relation [17]:

$$p_t = p + \varepsilon_0 \int_0^E \frac{\partial \varepsilon_s}{\partial T} dE \quad (2)$$

Variation of temperature generates the main pyroelectric effect, while the deformation of the active pyroelectric element and its non-uniform heating are generating the secondary and tertiary ones [17].

Equation (1) is changing for higher frequencies, when both $(\omega \tau_T)^2, (\omega \tau_e)^2 \gg 1$, $S \approx 1/\omega$, in the following simplified form:

$$S(\omega) = \frac{\eta p A P_{inc}}{\omega C_T C_e} \quad (3)$$

in which $C_T = \rho c A d$ and $C_e = A \varepsilon_0 \varepsilon_r / d$, considering the density (ρ), specific heat (c), vacuum permittivity (ε_0), static dielectric constant (ε_r), and the thickness (d) of the ferroelectric ceramic.

By definition, the voltage responsivity R_V is the ratio between the pyroelectric response in volts and the power of the laser diode in watts [8], there by presents a similar frequency dependence:

$$R_V = S/P_{inc} \quad (4)$$

According equations (3) and (4) after C_T and C_e substitution, the voltage becomes:

$$R_V = \frac{p}{\varepsilon_0 \varepsilon_r \rho c} \cdot \frac{\eta}{\omega A} \quad (5)$$

where $M = \frac{p}{\varepsilon_0 \varepsilon_r \rho c}$ is the figure of merit of the material, which can be estimated from the slope

of the $R_V = f\left(\frac{1}{\omega}\right)$ representation. The samples have the surfaces exposed to radiation covered with black absorber, which approximates its emissivity to one ($\eta \approx 1$). The figures of merit were calculated for samples with area $A = 9.62 \text{ cm}^2$ and two different thicknesses of $600 \text{ }\mu\text{m}$ and $250 \text{ }\mu\text{m}$

are $9.704 \cdot 10^{-3} \text{ m}^2/\text{C}$, and $11.64 \cdot 10^{-3} \text{ m}^2/\text{C}$ respectively. One can conclude that thinner active elements lead to larger figure of merits. However, such a result is unusual as the above relation for the figure of merit M contains only material constants thus, M should have the same value no matter the thickness. A possible explanation is that all these constants are for ideal crystals, while in real samples they may differ from sample to sample due to small differences in the structural quality even the composition is the same. For example, the amount of pores could be larger in thicker samples, leading to slightly smaller density. Apparently, this should lead to an increase in the value of M , which is not the case. This is because a larger porosity has impact on the success of the poling process, leading to a poorer poling and to a smaller pyroelectric response. Another advantage of thinner samples is that the maximum signal occurs at larger frequency, which might be important for applications requiring faster responses from the pyroelectric element.

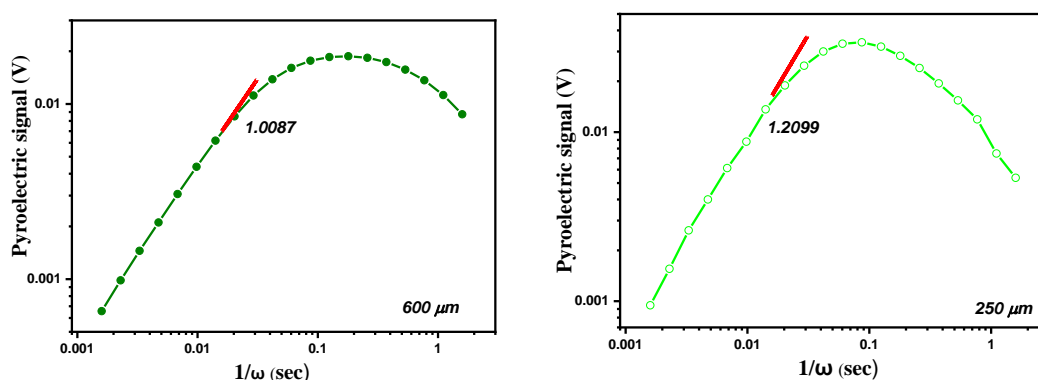


Fig. 5. R_V vs. $1/\omega$ representation for PBiZNFNT disks of different thicknesses.

4. Conclusions

$\text{Pb}_{0.98}\text{Bi}_{0.02}\text{Zr}_{0.5}\text{Fe}_{0.1}\text{Nb}_{0.09}\text{Ti}_{0.31}\text{O}_3$ (PBiZFNT) ceramic disks were obtained by the solid-state reaction method. SEM images reveal a compact structure, small porosity and uniform distribution of the perovskite grains. The magnitude of the pyroelectric signal is influenced by the thickness of the ceramic disk. It appears that the thinner is the disk the larger is the pyroelectric signal and the faster is the pyroelectric response, allowing operation at higher frequencies. In the present case, the optimum thickness is of 250 μm . This can be an useful information if one intends to use PBiZFNT ceramics as pyroelectric detectors for infrared radiations or application in laser pulse energy measurement.

Acknowledgements

The authors acknowledge funding through POC-G project MAT2IT (contract 54/2016, SMIS code 105726, Intermediary Body-Romanian Ministry of Research and Innovation), and the Core Program Core Program 2019-2022 (contract 21N/2019).

References

- [1] H. He, X. Lu, E. Hanc, C. Chen, H. Zhang, L. Lu, J. Mater. Chem. C **8**(5), 1494 (2020).
- [2] P. Duran, C. Moure, Mater. Chem. Phys. **15**(3), 193 (1986).
- [3] R. W. Whatmore, J. M. Herbert, F. W. Ainger, Phys. Status Solidi A **61**(1), 73 (1980).
- [4] R. W. Whatmore, Prog. Phys. **49**, 1335 (1986).
- [5] D. Damjanovic, Rep. Prog. Phys. **61**(9), 1267 (1998).

- [6] J. Wang, G. Wang, J. Wang, X. Chen et al., *Ceramics International* **142**, 10105 (2016).
- [7] A. Hizebry, H. Attaoui, M. Saadaoui, J. Chevalier, G. Fantozzi, *J. Eur. Ceram. Soc.* **27**, 557 (2007).
- [8] V. Stancu et al., *Process. Appl. Ceram.* **13**(3), 269 (2019).
- [9] L. Pintilie, I. Boerasu, M. Pereira, M. J. M. Gomes, *Mater. Sci. Eng. B* **109**(1), 174 (2004).
- [10] M. Botea, A. Iuga, L. Pintilie, *Appl. Phys. Lett.* **103** (23), 232902 (2013).
- [11] C. Chirila et al., *Plos One* **14**(8), e0221108 (2019).
- [12] E. Theocharous, C. Engtrakul, A. C. Dillon, J. Lehman, *Appl. Opt.* **47**(22), 3999 (2008).
- [13] J. Chen, Z. Xu, X. Yao, *Mater. Res. Innov.* **14**, 234 (2010).
- [14] A. Kumar and S. Mishra, *Adv. Mater. Lett.* **5**, 479 (2014).
- [15] C.-C. Hsiao, S.-Y. Liu, A.-S. Siao, *Sensors* **15**(7), 16248 (2015).
- [16] L. Pintilie, A. Iuga, V. Stancu, M. Botea, *Infrared Phys. Technol.* **106**, 103269 (2020).
- [17] A. Ianculescu et al., *Ceram. Int.* **42**(8), 10338 (2016).
- [18] R. W. Whatmore, *Rep. Prog. Phys.* **49** (12), 1335 (1986).
- [19] S. G. Porter, *Ferroelectrics* **33**(1), 193 (1981).